Ergod. Th. & Dynam. Sys. (2015), **35**, 1315–1344 © *Cambridge University Press, 2014*
doi:10.1017/etds.2013.100

Topological enumeration of complex polynomial vector fields

J. TOMASINI

Laboratoire Angevin de REcherche en MAthématiques (LAREMA), Université d'Angers, France
(e-mail: tomasini.jerome87@gmail.com)

(*Received* 18 *July* 2013 *and accepted in revised form* 27 *September* 2013)

Abstract. The enumeration of combinatorial classes of the complex polynomial vector fields in $\mathbb{C}$ presented by K. Dias [Enumerating combinatorial classes of the complex polynomial vector fields in $\mathbb{C}$. *Ergod. Th. & Dynam. Sys.* **33** (2013), 416–440] is extended here to a closed form enumeration of combinatorial classes for degree d polynomial vector fields up to rotations of the $2(d-1)$th roots of unity. The main tool in the proof of this result is based on a general method of enumeration developed by V. A. Liskovets [Reductive enumeration under mutually orthogonal group actions. *Acta Appl. Math.* **52** (1998), 91–120].

1. *Introduction*

In this work, our study is based on the equation

$$\dot{z} := \frac{dz}{dt} = Q(z), \quad t \in \mathbb{R},\ z \in \mathbb{C}, \tag{1}$$

where Q is a complex polynomial of degree $d \geq 2$. The set of trajectories of this equation partitions the complex plane following a particular pattern described by a simple combinatorial data set. The main goal of this article is to give a complete classification and enumeration of the topological structure of a vector field defined by a complex polynomial of degree d.

In the following, $\gamma(t, z)$ (or simply $\gamma(t)$ if the initial condition does not matter) will denote the solution of equation (1) passing through the point z, and we will define for all complex polynomial P

$$\xi_P(z) = P(z) \cdot \frac{d}{dz}$$

the polynomial vector field defined by P.

At first, as we are only interested in the topological structure of polynomial vector fields, we can consider that ξ_P and ξ_{-P} are topologically equivalent. In another way, it is easy to see that we can restrict our study to the set of monic, centered complex polynomial

https://doi.org/10.1017/etds.2013.100 Published online by Cambridge University Press

vector fields (i.e. the vector fields defined by a polynomial of the form $z^d + a_{d-2}z^{d-2} + \cdots + a_0$), in the sense that there exists an affine change of variable, uniquely determined by the multiplication of a $(d-1)$th root of unity, that changes the vector field defined by a complex polynomial Q of degree d to the vector field defined by a monic, centered complex polynomial P of degree d. Moreover, this change of variable does not change the topological structure of ξ_Q, i.e. ξ_Q and ξ_P are topologically equivalent. From now on we denote by $\mathcal{P}_d \simeq \mathbb{C}^{d-1}$ the set of monic, centered complex polynomials of degree d.

A recent study for the global classification of complex polynomial vector fields in $\mathbb{C}$, made first by Douady *et al* [**DES**] in the structurally stable (or generic) case, i.e. for polynomial vector fields such that there are neither homoclinic separatrices nor multiple equilibrium points, and then completed by Branner and Dias [**BD10**] for the general case, proved that a complex polynomial vector field in $\mathbb{C}$ is entirely determined by a combinatorial model (describing the topology of the vector field) and an analytic data set (describing the geometry of the vector field). More exactly, these two works show that for two given invariants (combinatorial and analytic), there exists a unique polynomial vector field defined by a monic, centered polynomial of fixed degree. In parallel to the work of Douady *et al*, Pilgrim gives in his article [**Pil06**] a method for explicitly constructing a generic, monic, centered polynomial P from any given combinatorial and a specific analytic data set.

We are often compelled in this article to consider the two situations, generic and non-generic polynomial vector fields, separately in order to simplify the presentation of the combinatorial models.

A natural question arising when we follow such work is how many different combinatorial models come from polynomial vector fields of fixed degree, which is equivalent to classifying our vector fields up to their topological structures. Part of this modeling and enumeration has already been done by Douady *et al* in the generic case, and was then enhanced by Dias in [**Dia13**] for the non-generic case, but these two strands do not exactly answer the original question in the sense that their modelization (and so a fortiori their enumerations) show a distinction between two polynomial vector fields which are conformally conjugate by a rotation. This distinction is due to the fact that the modelizations proposed in [**DES, Dia13**] impose an 'order' (symbolized by a marking in the combinatorial model) which is not specific to the vector fields.

The main contribution of this work is to find appropriate combinatorial models to enable the counting of the equivalent classes of polynomial vector fields without markings.

The contents of this paper are as follows. In §2, we introduce the main notions and basic facts about polynomial vector fields and we define two equivalence relations whose equivalence classes are the ones we want to count. In §3, we present four types of combinatorial models describing the topological structure of a polynomial vector field. The first three are combinatorial objects that already exist in the article [**DES**] for the generic case, and in [**Dia13**] for the non-generic case, but are necessary to introduce the last combinatorial model that fits our problem. Finally, in §4, we first give a general method, developed by Liskovets (see, for example, [**Lis98**]), in order to enumerate a set of unrooted planar maps. Thanks to this method, we will be able to prove the main results of this article.

https://doi.org/10.1017/etds.2013.100 Published online by Cambridge University Press

THEOREM 1.1. *The number σ_n of topological structures of generic complex polynomial vector fields of degree $d = n + 1$ is*

$$\sigma_n = \frac{1}{2n}\left[\frac{1}{n+1}\binom{2n}{n} + \sum_{\substack{l\geq 2\\ l|n}} \varphi(l)\binom{2n/l}{n/l} + \begin{cases}\dbinom{n}{\frac{n-1}{2}} & \text{if } n \text{ is odd}\\ 0 & \text{if } n \text{ is even}\end{cases}\right],$$

where φ is the Euler totient function. Moreover,

$$\lim_{n\to+\infty} (\sigma_n)^{1/n} = 4.$$

THEOREM 1.2. *The number p_n^+ of topological structures of complex polynomial vector fields of degree $d = n + 1$ is*

$$p_n^+ = \frac{1}{2n}\left[p_n + \sum_{\substack{l\geq 2\\ l|2n}} \varphi(l)\cdot\begin{cases}\sum_{k\geq 0} p_{n/l,k}\cdot(k+1) & \text{if } 2n/l \text{ is even}\\ c_{2n/l} & \text{if } 2n/l \text{ is odd}\end{cases}\right.$$
$$\left. + \begin{cases}0 & \text{if } n \text{ is even}\\ 2n\cdot p_{(n-1)/2} & \text{if } n \text{ is odd}\end{cases}\right], \quad n \geq 1,$$

with

$$p_{n,k} = \frac{(-2n)_k(-n)_k}{(2)_k}\frac{2^k}{k!}, \quad p_n = \sum_{k\geq 0} p_{n,k},$$

and

$$c_{2m+1} = -\sum_{k=0}^{m} a_k\left(\sum_{i=0}^{m-k}\alpha^i\beta^{m-k-i}\right),$$
$$c_{2m} = c_{2m+1} - 4\sum_{j=0}^{m-1} c_{2j+1}p_{m-j-1},$$

where α and β are the roots of the polynomial $X^2 + 11X - 1$, and

$$a_0 = -1, \quad a_1 = 4,$$
$$a_n = 6\sum_{k=0}^{n-2} p_k p_{n-2-k} - 2\sum_{k=0}^{n-2} p_k p_{n-1-k} + p_n \quad \text{for } n \geq 2.$$

Moreover,

$$\lim_{n\to+\infty} (p_n^+)^{1/n} = \frac{2}{5\sqrt{5}-11}.$$

The proof of this second theorem will be in three parts. In §4.3, we explain and give an explicit formula for the number p_n, then in §4.4 we prove Theorem 4.7, which is similar to Theorem 1.2 but with a recursive formula for the numbers c_n. Finally, in the last subsection, we give a closed formula for c_n.

https://doi.org/10.1017/etds.2013.100 Published online by Cambridge University Press

2. *Basic facts about polynomial vector fields*

Now we give a quick description of the main notions and definitions necessary to understand and to describe the combinatorial data set used in this article. For details about these results, see [**BD10, DES**].

A fundamental property of polynomial vector fields, which makes their study simpler, is that they do not have a limit cycle. This is a direct consequence of the following property.

PROPERTY 2.1. *Any accumulation point of a non-periodic orbit of ξ_P is a root of the polynomial P.*

In other words, for all non-periodic maximal solutions $\gamma(t, z)$ of ξ_P defined on the interval $]t_{\min}, t_{\max}[$:

- if $t_{\min} = -\infty$, $\gamma(t, z)$ tends to an equilibrium point of ξ_P as t tends to $-\infty$;
- if $t_{\max} = +\infty$, $\gamma(t, z)$ tends to an equilibrium point of ξ_P as t tends to $+\infty$;
- if $t_{\min}$ (respectively $t_{\max}$) is a finite number, $\gamma(t, z)$ tends to infinity as t tends to $t_{\min}$ (respectively $t_{\max}$).

Given $P \in \mathcal{P}_d$, let ζ be a root of the polynomial P. Then the vector field ξ_P associated with P admits an equilibrium point at the point ζ, and this equilibrium point can be one of the following four different types.

- ζ is a source if $\mathrm{Re}(P'(\zeta)) > 0$.
- ζ is a sink if $\mathrm{Re}(P'(\zeta)) < 0$.
- ζ is a center if $\mathrm{Re}(P'(\zeta)) = 0$ and $\mathrm{Im}(P'(\zeta)) \neq 0$.
- ζ is a multiple equilibrium point of multiplicity $m \geq 2$ if $P'(\zeta) = \cdots = P^{(m-1)}(\zeta) = 0$ and $P^{(m)}(\zeta) \neq 0$.

Each type of equilibrium point influences the global structure of the vector field in that a given equilibrium point ζ determines the behavior of the solutions passing through a neighborhood of it. This zone of influence is called the *basin*, denoted by $\mathcal{B}(\zeta)$, and is defined as follows.

- if ζ is a source, $\mathcal{B}(\zeta) = \{z \in \mathbb{C} \mid \gamma(t, z) \to \zeta \text{ for } t \to -\infty\}$.
- if ζ is a sink, $\mathcal{B}(\zeta) = \{z \in \mathbb{C} \mid \gamma(t, z) \to \zeta \text{ for } t \to +\infty\}$.
- if ζ is a center, $\mathcal{B}(\zeta) = \{\zeta\} \cup \{z \in \mathbb{C} \mid \gamma(t, z)$ is periodic and ζ is in the bounded component of $\mathbb{C}\backslash\gamma(\mathbb{R}, z)\}$.
- if ζ is a multiple equilibrium point, $\mathcal{B}(\zeta) = \mathcal{B}_\alpha(\zeta) \cup \mathcal{B}_\omega(\zeta) \cup \{\zeta\}$, where

$$\mathcal{B}_\alpha(\zeta) = \{z \neq \zeta \mid \gamma(t, z) \to \zeta \text{ for } t \to -\infty\} \quad \text{is the repelling basin,}$$
$$\mathcal{B}_\omega(\zeta) = \{z \neq \zeta \mid \gamma(t, z) \to \zeta \text{ for } t \to +\infty\} \quad \text{is the attracting basin.}$$

The connected components of $\mathcal{B}_\alpha(\zeta)$ and $\mathcal{B}_\omega(\zeta)$ are called repelling petals and attracting petals, respectively. In all four cases, $\mathcal{B}(\zeta)$ is an open, simply-connected domain containing ζ. See Figure 1 for an example showing the four different types of equilibrium point.

These tools already allow us better to understand the global structure of polynomial vector fields. In order to define this structure, a study of the vector field at infinity turns out to be the most interesting. In fact, for every polynomial $P \in \mathcal{P}_d$, there exists a unique $\mathbb{C}$-analytic isomorphism Φ, tangent to the identity at infinity, such that for each solution $\gamma_P(t, z)$ of ξ_P defined in a neighborhood of infinity there exists a solution γ of the vector

https://doi.org/10.1017/etds.2013.100 Published online by Cambridge University Press

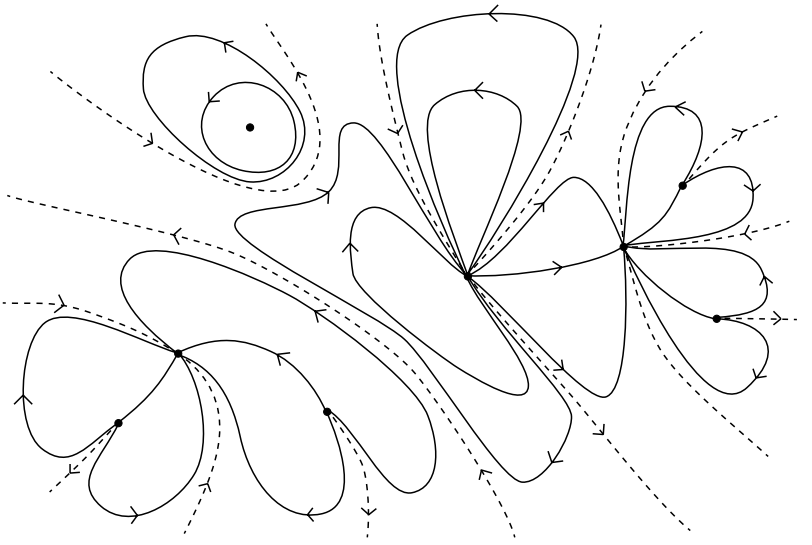


FIGURE 1. Example of a polynomial vector field of degree nine.

field ξ_d, defined by the polynomial z^d, such that

$$\Phi(\gamma_P(t, z)) = \gamma(t, \Phi(z)).$$

This relationship is also abbreviated as follows: $\Phi_*(\xi_P) = \xi_d$.

In other words, the behavior of the vector field ξ_P in a neighborhood of infinity is uniquely determined by the degree of the polynomial P. The study of the vector field ξ_d allows us to deduce that there exist $2d-2$ solutions γ_l, with $l \in \{0, \ldots, 2d-3\}$, of the polynomial differential equation $\dot{z} = P(z)$ defined in a neighborhood of infinity and asymptotic to the ray $t \cdot \delta_l$ for t large enough, where

$$\delta_l = \exp\left(\pi i \frac{l}{d-1}\right), \quad l \in \{0, \ldots, 2d-3\} \tag{2}$$

are the consecutive $2(d-1)$th roots of unity.

Moreover, if l is odd, there exists $\alpha_l \in]-\infty, 0[$ such that γ_l is defined on $]\alpha_l, 0]$ and $|\gamma_l(t)| \to \infty$ as $t \to \alpha_l$. Similarly, if l is even, there exists $\beta_l \in]0, +\infty[$ such that γ_l is defined on $]0, \beta_l[$ and $|\gamma_l(t)| \to \infty$ as $t \to \beta_l$. Then we call the *separatrices* of the vector field ξ_P, denoted by s_l, the maximal trajectories of ξ_P that coincide with the particular solutions γ_l. We distinguish the following three types of separatrix.

- s_l is an outgoing separatrix from the point at infinity if $\zeta := \overline{s}_l \backslash s_l$ is the limit point of s_l as t tends to $+\infty$ (this implies that l is odd).
- s_l is an incoming separatrix to the point at infinity if $\zeta := \overline{s}_l \backslash s_l$ is the limit point of s_l as t tends to $-\infty$ (this implies that l is even).
- s_l is a homoclinic separatrix of infinity if $\overline{s}_l \backslash s_l = \emptyset$ in $\mathbb{C}$. In this case, the separatrix s_l is both outgoing from and incoming to infinity, so this maximal trajectory is defined by two particular solutions γ_k and γ_j, with k odd and j even. In this case, $l = k$ or j, which is why we also denote $s_l = s_{k,j}$.

https://doi.org/10.1017/etds.2013.100 Published online by Cambridge University Press

These trajectories are the only ones which tend to infinity. Note that the way we present the separatrices here imposes a label, and so an order between these solutions. This is the main issue of the enumeration presented in this article.

The *separatrix graph* (or configuration) Γ_P of ξ_P is defined as follows:

$$\Gamma_P = \bigcup_{l=0}^{2d-3} \widehat{s_l},$$

where $\widehat{s_l}$ is the closure of s_l in the Riemann sphere $\widehat{\mathbb{C}}$.

The separatrix graph is an important tool for our study. In fact, the global phase portrait of a polynomial equation (1) is univocally determined by its separatrix graph, in the sense that the separatrix graph can be used to identify the topological structure of polynomial vector fields. According to that result, in order to give a topological enumeration of complex polynomial vector fields, we need to know how many separatrix graphs we can construct (up to equivalence).

Now, let Γ_P be the separatrix graph on the compactification of $\mathbb{C}$ associated with the polynomial P, and embed it into the closed unit disk $\overline{\mathbb{D}}$ so that the point at infinity is sent to the unit circle, i.e. it performs a blowing up of the sphere at the point ∞. The interest of such an embedding is to highlight the common property of polynomial vector fields in a neighborhood of infinity, i.e. the directions of the separatrices to infinity. Consider $\mathbb{S}^1$ as the disjoint union of half-closed intervals $\tilde{E}_j = \{e^{2\pi i t}, t \in]\theta_{j-1}, \theta_j]\}$, where $\theta_j = j/2(d-1)$, and E_j is the interior of $\tilde{E}_j$. The half-closed intervals $\tilde{E}_j$ are called the *boards* of the unit disk.

Let Z be a connected component of $\overline{\mathbb{D}}\backslash\Gamma_P$ (where the separatrix graph Γ_P is embedded in $\overline{\mathbb{D}}$). Such a component is called a *zone* and can be of the three following different types.

(1) There is no equilibrium point on the boundary ∂Z. In this case, Z is called a *center zone* that contains a center, and all trajectories in Z are periodic (with the same period). Moreover, the boundary of Z consists of one or several homoclinic separatrices, and if a center zone contains k homoclinic separatrices on the boundary ∂Z, then the center zone intersects $\mathbb{S}^1$ at k open arcs $E_{i_1}, \ldots, E_{i_k}$.

(2) There is exactly one equilibrium point on the boundary ∂Z. Then this equilibrium point is necessarily a multiple equilibrium point ζ. In this case, $Z = \mathcal{B}_\alpha(\zeta) \cap \mathcal{B}_\omega(\zeta)$, is called a *sepal zone*. There are exactly $2m-2$ sepals corresponding to a multiple equilibrium point of multiplicity m. Moreover the boundary of Z contains exactly one incoming and one outgoing separatrix, and possibly one or several homoclinic separatrices. If a sepal zone contains k homoclinic separatrices on its boundary, then it intersects $\mathbb{S}^1$ at $k+1$ open arcs.

(3) There are exactly two equilibrium points ζ_α and ζ_β on the boundary ∂Z. In this case, Z contains no equilibrium point inside. It is called an *$\alpha\omega$-zone* and is one of the following four subtypes.
   - $Z = \mathcal{B}(\zeta_\alpha) \cap \mathcal{B}(\zeta_\omega)$, where ζ_α and ζ_ω are a source and a sink, respectively.
   - $Z = \mathcal{B}(\zeta_\alpha) \cap \mathcal{B}_\omega(\zeta_\omega)$, where ζ_α and ζ_ω are a source and a multiple equilibrium point respectively. In this case Z is called an attracting interpetal for ζ_ω.

https://doi.org/10.1017/etds.2013.100 Published online by Cambridge University Press

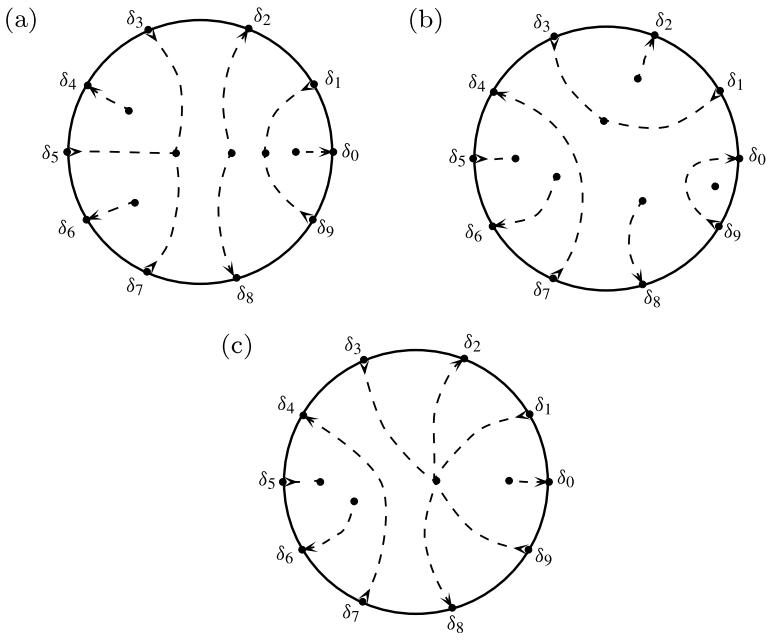


FIGURE 2. Example of separatrix graphs. (a) A generic case. (b) A case with two homoclinic separatrices which link δ_0 and δ_9, and δ_4 and δ_7. (c) A case with a multiple point of order three.

- $Z = \mathcal{B}_\alpha(\zeta_\alpha) \cap \mathcal{B}(\zeta_\omega)$, where ζ_α and ζ_ω are a multiple equilibrium point and a sink respectively. In this case Z is called a repelling interpetal for ζ_α.
- $Z = \mathcal{B}_\alpha(\zeta_\alpha) \cap \mathcal{B}_\omega(\zeta_\omega)$, where ζ_α and ζ_ω are both multiple equilibrium points. In this case Z is a repelling interpetal for ζ_α and an attracting interpetal for ζ_ω.

The boundary of Z contains one or two incoming separatrices and one or two outgoing separatrices, and possibly one or several homoclinic separatrices. Moreover, if Z is both on the left of k (oriented) homoclinic separatrices and on the right of l (oriented) homoclinic separatrices on its boundary, then Z intersects $\overline{\mathbb{D}}$ at $k+1$ odd open arcs and $l+1$ even open arcs.

We can finally give simple definitions of the two equivalence relations necessary for our enumeration.

Definition 2.2. Let P, Q be two monic, centered polynomials of degree d, and Γ_P, Γ_Q be their respective separatrix graphs. We say that the two polynomial vector fields ξ_P and ξ_Q are equivalent, denoted by $P \sim Q$, if there exists an isotopy $h : \overline{\mathbb{D}} \times [0, 1] \to \overline{\mathbb{D}}$ that sends the separatrices of Γ_P to the separatrices of Γ_Q and such that $h_{|S^1 \times [0,1]} = \mathrm{id}$.

Definition 2.3. Let P, Q be two monic, centered polynomials of degree d, and Γ_P, Γ_Q be their respective separatrix graphs. We say that the two polynomial vector fields ξ_P and ξ_Q are topologically equivalent, denoted by $P \sim_{\mathrm{top}} Q$, if there exists an isotopy $h : \overline{\mathbb{D}} \times [0, 1] \to \overline{\mathbb{D}}$ that sends the separatrices of Γ_P to the separatrices of Γ_Q (cf. Figure 3 for an example).

https://doi.org/10.1017/etds.2013.100 Published online by Cambridge University Press

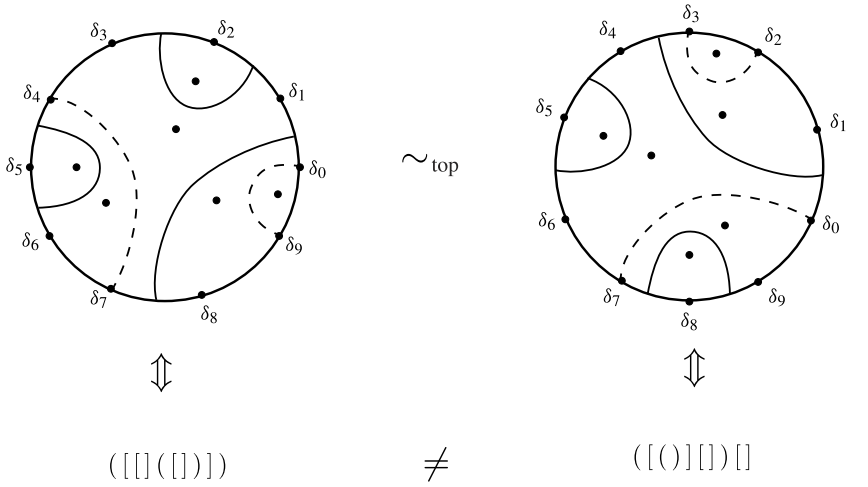


FIGURE 3. Examples of two topologically equivalent vector fields with different bracketing representations.

3. *Combinatorial models*

In this section, we introduce various combinatorial models which will enable us to enumerate the equivalence classes of the complex polynomial vector fields. The first models studied in this section are similar to those already present in the articles [**DES, Dia13**]. The interested reader can refer to these articles for more details.

3.1. *From separatrix graph Γ_P to transversal graph Σ_P.* Let P be a monic centered polynomial of degree d, and Γ_P be its separatrix graph. Then using the different known information about the connected components of $\overline{\mathbb{D}}\backslash\Gamma_P$ given in the previous section, we can construct a new combinatorial data set. For this, we distinguish the following two important types of object.

(1) *Homoclinic separatrices*. These particular solutions of our polynomial differential equation link two points δ_i and δ_j at infinity (such a solution is usually denoted by $s_{i,j}$), and so link boards $\tilde{E}_i$ and $\tilde{E}_j$;

(2) *$\alpha\omega$-zones*. Such a zone is equivalent to a band, having exactly one even boards $\tilde{E}_i$ and one odd boards $\tilde{E}_j$ not still linked with another boards by a homoclinic separatrix. So we can trace a curve, contained in the zone, between E_i and E_j such that it does not cross any separatrices and crosses the trajectories of ξ_P at a constant, non-zero angle. This curve is called transversal and denoted by $T_{i,j}$. Notice that the transversal $T_{i,j}$ pairs the boards $\tilde{E}_i$ and $\tilde{E}_j$.

So, starting from a separatrix graph Γ_P, we construct a new graph on the unit disk, called the transversal graph and denoted by Σ_P, defined by the union of the transversals and the homoclinic separatrices coming from Γ_P. Note that this graph is constructed by pairing even board $\tilde{E}_i$ with odd board $\tilde{E}_j$. Nevertheless, some boards are not paired with others; these boards are those derived from sepal zones. See Figure 4 for some examples.

One of the remarkable properties due to the construction of these graphs is that each connected component of the disk bounded by Σ_P contains one and only one equilibrium

https://doi.org/10.1017/etds.2013.100 Published online by Cambridge University Press

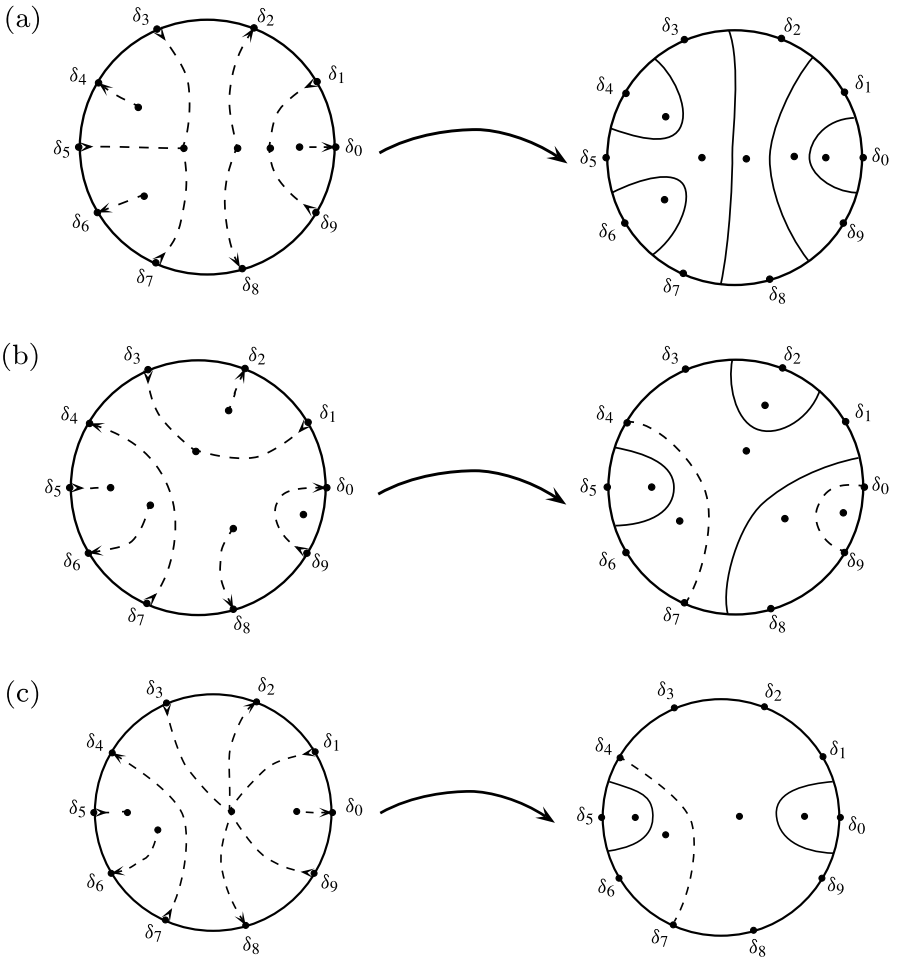


FIGURE 4. Examples of separatrix graphs and their respective transversal graphs, where separatrices are drawn with dashed curves and transversals are drawn with solid curves. (a) A generic case. (b) A case with homoclinic separatrices. (c) A case with a multiple point.

point of the polynomial vector field ξ_P. So it is easy to reconstruct the separatrix graph Γ_P from the associated transversal graph Σ_P. In other words, we have a bijection between the set of separatrix graphs and the set of transversal graphs.

Moreover, the reader can see that for $P, Q \in \mathcal{P}_d$, $P \sim Q$ if and only if they have the same transversal graph, i.e. Σ_P and Σ_Q are constructed by pairing the same boards. Similarly, $P \sim_{\text{top}} Q$ if and only if there exists $l \in \{0, \ldots, 2d-3\}$ such that Σ_Q is obtained by a rotation of Σ_P of order $l/(2d-2)$ (see Figure 3 for an example).

In summary, in order to count the number of equivalent phase portraits of the polynomial differential equations $\dot{z} = P(z)$, we have to enumerate the number of transversal graphs, i.e. the number of different ways to pair the $2d-2$ boards of $\overline{\mathbb{D}}$. A first enumeration of this problem was given by Douady *et al*, who classified the structurally stable (or generic) case, i.e. the vector fields such that there are neither homoclinic separatrices nor multiple

https://doi.org/10.1017/etds.2013.100 Published online by Cambridge University Press

equilibrium points. Later this result was completed, thanks to the introduction of a new combinatorial, by the classification of the global structures of complex polynomial vector fields in $\mathbb{C}$. This generalization is due to a work of Branner and Dias [**BD10**].

3.2. *From transversal graphs to valid bracketings.* First let me explain the idea developed by Dias in [**Dia13**]. This idea is to translate the combinatorial data set defined by the transversal graphs into a simpler bracketing problem in order to facilitate the enumeration of general polynomial vector fields. The bracketing problem proposed here is not exactly the same as the one proposed by Dias, but it is an equivalent problem. Consider a string of $2d-2$ elements including the integers from 0 to $2d-3$, and use the following rules.

(1) For each homoclinic separatrix $s_{i,j}$ of the transversal graph, replace the integers i and j by left and right brackets, respectively, i.e. $i-1\ (\ i+1\ldots j-1\ )\ j+1$. These pairs of brackets are called associated.
(2) For each transversal $T_{k,l}$ of the transversal graph, replace the integers k and l by square bracket, i.e. $k-1\ [\ k+1\ldots l-1\ ]\ l+1$. These pairs of brackets are called associated.
(3) For each board $\tilde{E}_i$ that is not connected to another one, replace the integer i by a dot, i.e. $i-1\bullet i+1$.

In this way, a transversal graph induces a unique bracketing representation. For example, the respective bracketing representations of the examples (a)–(c) of Figure 4 are respectively [ ] [[[ ] [ ]]], ([[ ] ([ ])]) and [ ] • • ([ ]) • •. Figure 3 gives also an example of translation from transversal graphs to valid bracketings. Note that we can also write a valid bracketing with the elements of the string (as Dias did in her paper). For example, we can write [01][23]4(56)7 instead of [ ] [ ] • ( ) •.

Conversely, the bracketing representation must satisfy some properties so that they are in accordance with what can happen for a given polynomial vector field (and so for the associated transversal graph). For that, we need to impose some rules on how to place the elements of a bracketing representation. So, consider a bracketing representation containing $2d-2$ elements. It is called a *valid bracketing* if it has the following properties.

(1) There are an equal number of right and left round and square brackets.
(2) The number of left square (respectively round) brackets must be greater than or equal to the number of right, reading from left to right.
(3) There must be an even number of brackets and dots between a pair of round (respectively square) associated brackets.
(4) There must be an equal number of right and left square (respectively round) brackets between a pair of (round or square) associated brackets.

So, we create a bijection between the set of transversal graphs and the set of valid bracketings. Notice that the structurally stable case of vector fields (containing neither homoclinic separatrices nor sepal zones) is equivalent by this transformation to the classical bracketing problem, whose enumeration is given by the Catalan numbers [**Dav12**].

Thanks to this combinatorial, given first in the work of Branner and Dias [**BD10**], we can enumerate the equivalence classes defined by the relation $\sim$. This enumeration

https://doi.org/10.1017/etds.2013.100 Published online by Cambridge University Press

is given in Lemma 4.5, and is proved first by Dias in [**Dia13**]. The main problem of this point of view is the following: this combinatorics depends on the enumeration of the points δ_l on the unit circle. In fact, Figure 3 shows an example of two topologically equivalent transversal graphs (one is obtained by a rotation of the other) having different respective bracketing representations. In other words, the problem here is that it is difficult to identify topologically equivalent polynomials using this combinatorics. In order to solve this difficulty, we will give in the next subsection another equivalent combinatorial data set. Before that, we give a generalization of the concept of valid bracketing defined for an odd number of elements in the string.

Consider a bracketing representation of n elements, not necessarily even. It is called a *valid bracketing* if it satisfies properties 1, 2 and 4 of the previous definition, and also the following property.

(3) There must be an even number of brackets and dots between a pair of round (respectively square) associated brackets, *except maybe one*.

This notion of valid bracketing containing an odd number of elements has no relation to polynomial vector fields, but will be useful later.

3.3. *A step towards trees.* The purpose of this subsection is to show a link between all combinatorial forms (transversal graphs, valid bracketings) presented so far in this article and a more general concept of trees. How we present this link will be very close to what can be found in the article of Pilgrim [**Pil06**], who made the connection between transversal graphs and combinatorial objects called Grothendieck dessins d'enfants. This presentation will be an opportunity to propose a simple encoding of the combinatorics we have worked with so far. In the following, we treat the situations with multiple points and the situations without multiple points separately. But before that, we will return next to some basic notions about planar maps.

A *planar graph* is a graph that can be drawn in $\mathbb{R}^2$ without edge-crossing. A *planar map* is a proper embedding of a connected graph into the two-dimensional sphere considered up to orientation preserving homeomorphisms of the sphere. In other words, a planar map is a connected planar graph drawn in the sphere considered up to continuous deformation. So the difference between a map and a graph is that a map has vertices and edges (like a graph), but also faces. From the topological point of view, a planar graph is a CW complex of dimension one whereas a planar map is a CW complex of dimension two.

We will finish this introduction by the definition of a rooted planar map. Figure 5 shows an example of a rooted map.

Definition 3.1. A planar map is called *rooted* by distinguishing an oriented edge. The original vertex of this distinguished oriented edge is called the root vertex of the map.

3.3.1. *Case without multiple points.* Now, back to our combinatorial description. First consider a transversal graph Σ associated with a polynomial vector field of degree d without multiple points, i.e. for every index $i \in \{0, \dots, 2d-2\}$ there exists an index $j \in \{0, \dots, 2d-2\}$, $j \neq i$, so that the boards $\tilde{E}_i$ and $\tilde{E}_j$ are connected by a transversal $T_{i,j}$ or by a homoclinic separatrix $s_{i,j}$. From the results reported in the second section of the article, we deduce that the graph Σ splits the closed unit disk $\overline{\mathbb{D}}$ into d areas whose

https://doi.org/10.1017/etds.2013.100 Published online by Cambridge University Press

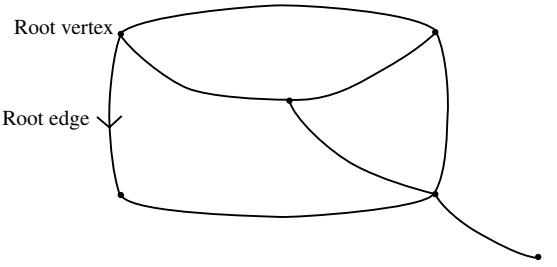


FIGURE 5. Example of a rooted planar map.

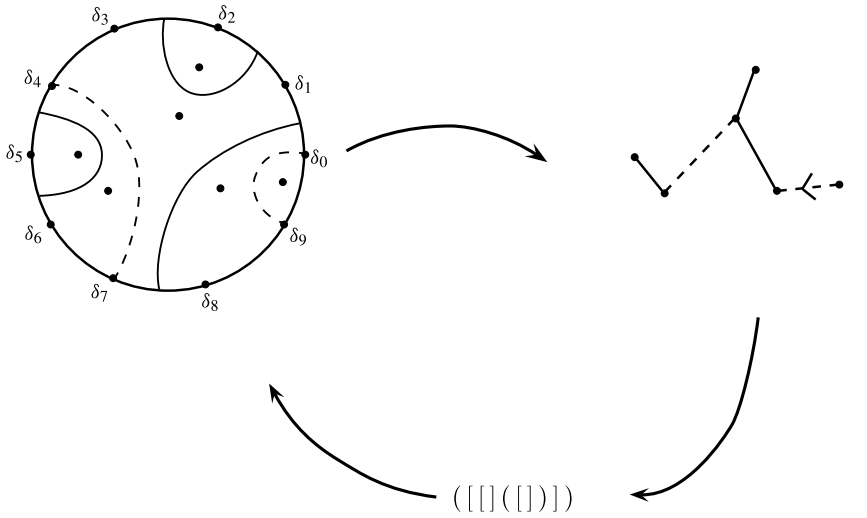


FIGURE 6. Example of equivalence between a transversal graph without multiple points and its respective valid bracketing and rooted generalized tree.

boundaries consist of transversals and homoclinic separatrices. Subsequently, we say that two areas are *adjacent* if their respective boundaries share a transversal or a homoclinic separatrix. The construction of an associated planar map $\mathcal{T}$ is then natural. First, in each area is arranged a vertex and then two vertices are connected to each other if their respective areas are adjacent. More precisely, two vertices are connected by a continuous edge (respectively dotted edge) if the boundaries of their respective areas share a common transversal (respectively homoclinic separatrix). See Figure 6 for an example.

It is easy to see that the planar map $\mathcal{T}$ obtained is a map with only one face seeing it as the dual map of the transversal graph Σ on the sphere. These particular maps are called planar trees (or just trees). Notice that our trees have the particularity of being defined by distinguishing two types of edge. Now, we need to translate the numeration of boards $\tilde{E}_i$. For that, we will root our tree. Consider the oriented transversal $T_{0,j}$ (respectively homoclinic separatrix $s_{0,j}$), i.e. the transversal (respectively homoclinic separatrix) comes from $\tilde{E}_0$ to $\tilde{E}_j$, and denote by x_0 the vertex of $\mathcal{T}$ to the left of this transversal (respectively homoclinic separatrix). This vertex will be the root vertex of the tree.

https://doi.org/10.1017/etds.2013.100 Published online by Cambridge University Press

Similarly, consider the oriented transversal $T_{1,k}$ (respectively homoclinic separatrix $s_{1,k}$), and denote by x_1 the vertex of $\mathcal{T}$ to the left of this transversal (respectively homoclinic separatrix). Then we define the root of the tree as the edge from x_0 to x_1.

So, we get an application that transforms a given transversal graph into a rooted tree. Conversely, consider a rooted tree $\mathcal{T}$ as defined above, we will show by another construction that this tree is linked to a valid bracketing (the same valid bracketing describing the transversal graph Σ which comes from the tree).

From the root vertex, and following the direction given by the root, we will follow the contour of the tree in the counterclockwise direction, stopping at each vertex encountered. In doing so, we will go through each edge exactly twice. So, following the contour defined later, we will write in a string of elements a left square bracket '[' whenever a continuous edge is passed for the first time, and a right one ']' whenever a continuous edge is passed for the second time. Similarly, we will write in the same string a left round brackets '(' whenever a dotted edge is passed for the first time, and a right one ')' whenever a dotted edge is passed for the second time. This is a classical encoding for trees. See [**BM96**] for more details on this encoding.

It is easy to see that this transformation constructs a valid bracketing. It is left to the reader to verify that the valid bracketing obtained thanks to the rooted tree is the same as that obtained directly through the transversal graph Σ. An example is given at Figure 6.

3.3.2. *Case with multiple points.* Now, consider a transversal graph Σ' associated with a polynomial vector field of degree d with multiple point(s), i.e. there is at least one index $i \in \{0, \ldots, 2d-2\}$ such that the board $\tilde{E}_i$ is not connected to another one. In this case, the graph Σ' splits the closed unit disk into $k < d$ areas whose boundaries consist of transversals and homoclinic separatrices. First, we perform the same construction as in the previous case: in each area is arranged a vertex and two vertices are connected by a continuous (respectively dotted) edge to each other if their respective areas share a common transversal (respectively homoclinic separatrix). Then, we must take in consideration the boards which are not connected to other boards. It is important to notice that each of these boards is entirely contained in an area. So, we can draw a (continuous) edge from a point of a board which is not connected to another one to the vertex associated with the area containing this board. In this case, our map $\mathcal{T}'$ has the particularity of having some edges connected by only one vertex. These edges are called *half-edges*.

So, from the transversal graph Σ', we construct a planar map $\mathcal{T}'$, similar to the previous one, which contains some half-edges. In the following, these trees will be called *generalized trees*. As above, now we will root the map $\mathcal{T}'$ as follows: denote by x_0 the vertex defined as the vertex to the left of the oriented transversal $T_{0,j}$ (respectively homoclinic separatrix $s_{0,j}$) or as the vertex associated with the area containing entirely the end $\tilde{E}_0$ if $\tilde{E}_0$ is not connected to another end. This vertex will be the root vertex of the tree $\mathcal{T}'$. Similarly, denote by x_1 the vertex defined as the vertex to the left of the oriented transversal $T_{1,k}$ (respectively homoclinic separatrix $s_{1,k}$) or as the vertex associated with the area containing entirely the end $\tilde{E}_1$. Then we define the root of $\mathcal{T}'$ as the edge from x_0 to x_1.

https://doi.org/10.1017/etds.2013.100 Published online by Cambridge University Press

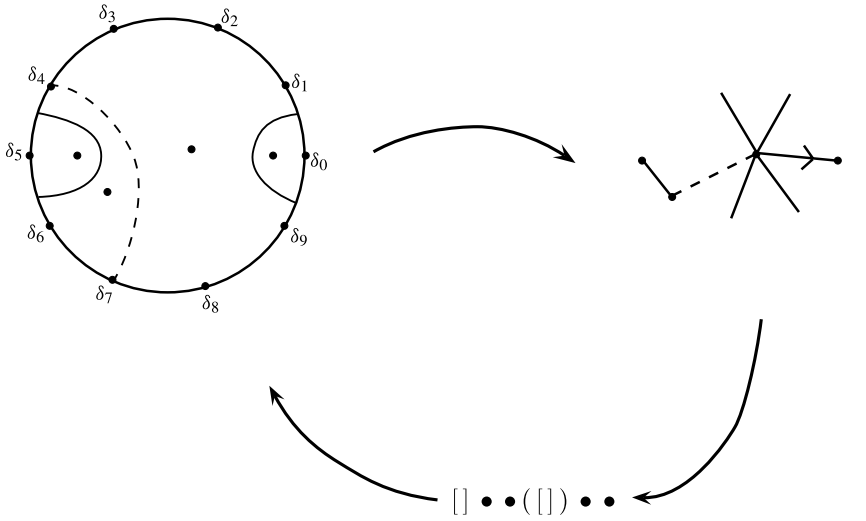


FIGURE 7. Example of equivalence between a transversal graph with a multiple point and its respective valid bracketing and rooted generalized tree.

Conversely, consider a rooted generalized tree $\mathcal{T}'$. We will use the same encoding as before with only one difference. Because of the existence of half-edges, it is possible, when we follow the contour of the map, to go from a vertex to itself. In this case, we will simply add a unique dot • in the string of elements. In other words, we will suppose that half-edges are passed only once (and not twice as for edges). Through the same transformation as above, it is easy to see that this encoding is equivalent to a valid bracketing and that the valid bracketing obtained thanks to $\mathcal{T}'$ is the same as that obtained directly through the transversal graph Σ'. An example is given at Figure 7.

In conclusion, we have established a bijection between the set of transversal graphs and the set of rooted generalized trees. By taking quotients we also obtain a bijection between the set of transversal graphs quotiented by the group generated by a rotation of the unit circle of order $1/(2d-2)$ and the set of unrooted generalized trees.

In the following, a generalized tree will be of order n if the number of edges plus half the number of half-edge is equal to n, i.e. a *generalized tree of order n* is a generalized tree having k edges and $2(n-k)$ half-edges for k between 0 and n.

4. *Enumeration*

4.1. *A method for enumerating unrooted maps.* The results of the last section imply that counting the number of polynomial vector fields to topological equivalence amounts to counting the number of unrooted generalized trees. In general, enumerating unrooted maps is a difficult problem due to the presence of various symmetries. Here, we use a method developed by Liskovets to overcome this difficulty. Only the main arguments of this method will be given; for more details, see [**Lis96, Lis98**]. The interested reader can also see [**Lis96**] for an application and [**Lis04**] for some results obtained thanks to that method. Notice that the results we use here are extensions of results proved by Liskovets

https://doi.org/10.1017/etds.2013.100 Published online by Cambridge University Press

because we work with a generalized concept of maps, due to the presence of half-edges, but the demonstrations of these results are the same. In the following, we only work with a concept of generalized maps.

For the problem under consideration, let $\mathcal{M}$ be a certain set of maps described in a given surface, and let $\mathcal{M}(n) \subset \mathcal{M}$ be the subset of $\mathcal{M}$ containing all maps of $\mathcal{M}$ with exactly n edges ($n \geq 2$). Moreover, we suppose that the surface where we construct our maps is orientable and has a given orientation. Then we can calculate the number of unrooted maps knowing the number of l-rooted maps (see Definition 4.2). More precisely, we have the following result.

THEOREM 4.1.

$$M^{+}(n) = \frac{1}{2n} \sum_{\substack{l \geq 1 \\ l \mid 2n}} \varphi(l) \cdot M^{(+,l)}(n), \quad n \geq 2,$$

where $M^{+}(n)$ (respectively $M^{(+,l)}(n)$) is the number of non-isomorphic (respectively l-rooted) maps in $\mathcal{M}(n)$ considered up to orientation-preserving homeomorphisms and φ is the Euler totient function.

Notice that $M^{(+,1)}(n)$ is simply the number of rooted maps in $\mathcal{M}(n)$; this set is generally denoted by $M'(n)$. We will use this notation in the following.

This theorem, obtained thanks to some algebraic results on the group action theory, is true in all orientable surfaces, but has a more interesting interpretation in the case of the sphere S^2. In fact, according to a result of Mani [**Man71**], any planar map may be represented on the (geometrical) sphere in such a way that all its automorphisms are induced by symmetries of the sphere. On the other hand, as we only consider up to orientation-preserving automorphisms, this result implies that all symmetries of a given planar map, described on the sphere with a good representation, can be deduced by rotations of the sphere. This observation will induce later the concept of quotient maps, which will be very useful for enumerating l-rooted maps, which is at first sight a difficult problem. But first we need to define the notion of an l-rooted map.

Definition 4.2. An l-rooted map is a map with l rooted edges that exhibits a symmetry of order l (with respect to the roots).

The definition of l-rooted maps is a natural generalization of the concept of rooted maps introduced in Definition 3.1. The reader can find an example of a 3-rooted map in Figure 8 and an example of a 2-rooted map in Figure 9.

Now let us return to the concept of quotient maps mentioned earlier. We will define this notion from a geometrical point of view. Let A be a planar map admitting a symmetry of order l, and consider a representation of this map on the sphere such that the symmetry of A is induced by a rotation ρ of the sphere of order l. Then, we construct the *quotient map* B of A, with respect to the rotation ρ, by cutting out a spherical sector with angle $2\pi/l$ bearing upon the poles (i.e. the intersection between the rotation axis and the sphere) and then by glueing its boundary half-circles to form a sphere so that the quotient map is also a planar map. Figure 10 shows an example of the construction of a quotient map. For the sake of clarity, other examples of quotient maps will be represented on the plane.

https://doi.org/10.1017/etds.2013.100 Published online by Cambridge University Press

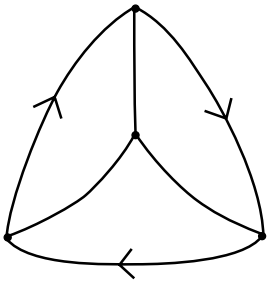


FIGURE 8. Example of a 3-rooted planar map.

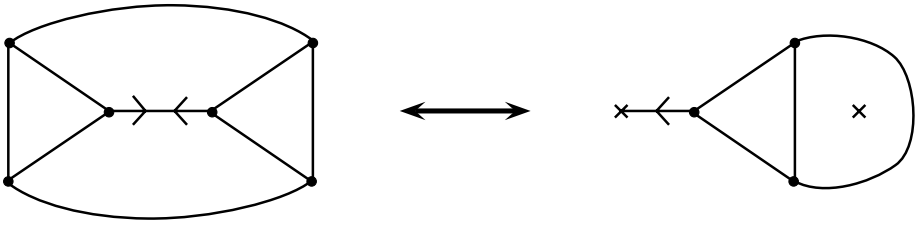


FIGURE 9. Example of a 2-rooted map and its quotient map.

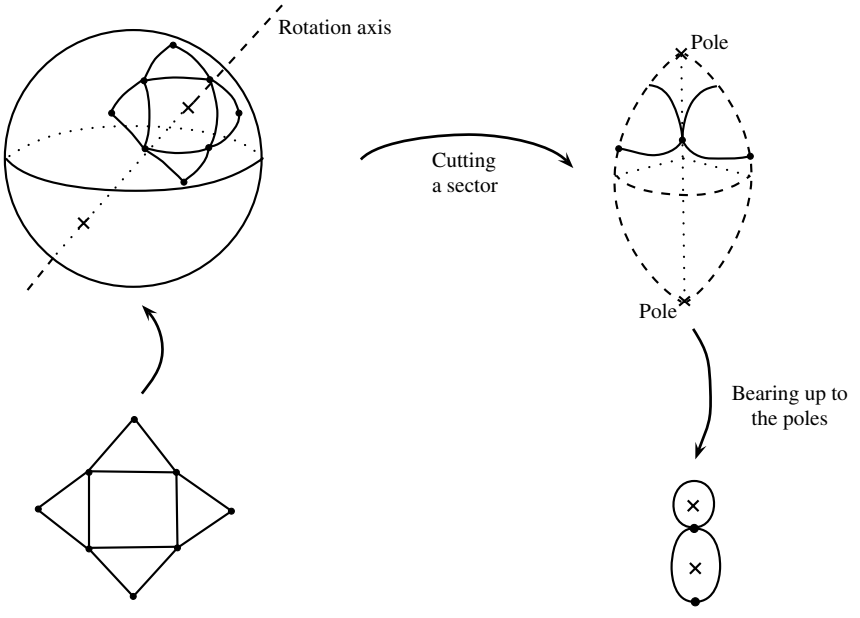


FIGURE 10. Example of a construction of a quotient map with two axial faces.

https://doi.org/10.1017/etds.2013.100 Published online by Cambridge University Press

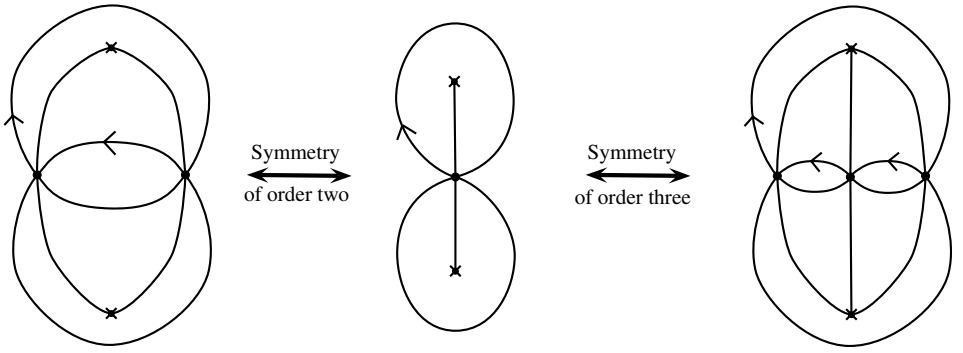


FIGURE 11. Example of a quotient map with two axial vertices and its associated 2-rooted map (left) and 3-rooted map (right).

Notice that the quotient map is independent of the choice of the sector because of the symmetry of the map A. Moreover, if A is rooted, then we will choose a sector that contains the root, so that the quotient map B is also rooted. Similarly, if A is an l-rooted map, its quotient map, with respect to the symmetry of A of order l, is a rooted map (due to the definition of a l-rooted map, which implies that each sector contains one and only one root of the map A). In particular, it is for this reason that the concept of quotient map will be a great help later.

Notice also that the poles of the map A are still contained on the quotient map B. The vertices, edges or faces (called cells) of the map A (respectively the vertices, half-edges or faces of the quotient map B) which contain these poles are called *axial*.

The reader may also notice that the quotient of a tree is always a tree. In fact, by definition, a quotient has necessarily fewer faces than the map from which it is derived, which is why the quotient of a tree has only one face, and so it is a tree.

Conversely, we want to reconstruct the initial planar map A knowing its quotient map B. This construction is a simple one from the moment when we know the axial cells of B and the order l of the rotation used to create the quotient map. In fact, by knowing this information, we can represent on the sphere the quotient map B such that the two axial cells of B are placed on the north and south poles of the sphere. Then by cutting the sphere relative to a half-circle from the north pole to the south pole, we can open the sphere until we obtain a sphere sector with angle $2\pi/l$. Finally, by glueing l copies of this sphere sector, we construct a planar map which is exactly the map A. Figure 11 shows an example of this construction.

The only exception to this construction is when the quotient map has an axial half-edge. In this case, the order l of the symmetry is fixed at two. See Figure 9 for an example. It is for this reason that for our enumeration we will distinguish two cases: the quotient map having an axial half-edge, and the quotient map without an axial half-edge. The first case is often more difficult to enumerate.

Remark. The notion of l-rooted map can be defined for a bracketing representation. In fact, we say that a bracketing representation of n elements is l rooted if it is constructed by copying the same string of n/l elements l times. The quotient associated with this bracketing is simply the string of n/l elements.

https://doi.org/10.1017/etds.2013.100 Published online by Cambridge University Press

Now, thanks to this concept of quotient maps, we can rewrite Theorem 4.1 as follows.

THEOREM 4.3. (Liskovets)

$$M^+(n) = \frac{1}{2n}\left[M'(n) + \sum_{\substack{l\geq 2 \\ l|2n}} \varphi(l)\cdot M'_l(n) + M'_e(n)\right], \quad n \geq 2,$$

where $M'(n)$ is the number of rooted maps of $\mathcal{M}(n)$, $M'_e(n)$ is the number of rooted quotient maps from 2-rooted maps of $\mathcal{M}(n)$ with an axial half-edge, and $M'_l(n)$ is the number of rooted quotient maps from l-rooted maps without axial half-edge.

4.2. *A first application: the generic case.* In this subsection, we will use the example of structurally stable polynomial vector fields described by Douady *et al* in [**DES**] to explain Theorem 4.3 in a simple case. In fact, in this case, the bracketing problem is equivalent to the enumeration of rooted trees, also the number σ_n of topologically equivalent phase portraits of generic complex polynomial differential equations (of degree $d = n+1$) is equal to the number $T^+(n)$ of unrooted trees (with n edges). So, in order to prove Theorem 1.1, we have to prove first that

$$\sigma_n = T^+(n) = \frac{1}{2n}\left[\frac{1}{n+1}\binom{2n}{n} + \sum_{\substack{l\geq 2 \\ l|n}} \varphi(l)\binom{2n/l}{n/l} + \begin{cases} \dbinom{n}{\frac{n-1}{2}} & \text{if } n \text{ is odd} \\ 0 & \text{if } n \text{ is even} \end{cases} \right].$$

This result can also be found in [**Lis04**]. Notice also that we obtain the same result in the case of complex polynomial vector fields where all equilibrium points are centers. The interested readers can refer to the article [**AGP10**] for more details about this particular case.

Now let us solve the enumeration problem of unrooted trees using Theorem 4.3. This theorem applied to our situation gives that

$$T^+(n) = \frac{1}{2n}\left[T'(n) + \sum_{\substack{l\geq 2 \\ l|2n}} \varphi(l)\cdot T'_l(n) + T'_e(n)\right], \quad n \geq 2,$$

where $T'(n)$ is the number of rooted trees, $T'_e(n)$ is the number of rooted quotient trees with an axial half-edge, and $T'_l(n)$ is the number of rooted quotient trees without axial half-edge obtained thanks to a symmetry of order l.

The enumeration of rooted trees was obtained a long time ago, and the solution of this problem is given by the numbers of Catalan (see [**Dav12**] for more details). So,

$$T'(n) = \frac{1}{n+1}\binom{2n}{n}.$$

It remains to determinate the values $T'_l(n)$ and $T'_e(n)$. For that, we need to understand the quotient maps obtained from trees, and more particularly the set of pairs of axial cells involved in this quotient action. In a general study, there are the following six different pairs.

https://doi.org/10.1017/etds.2013.100 Published online by Cambridge University Press

- The two axial cells are vertices (see Figure 11).
- The two axial cells are edges.
- The two axial cells are faces (see Figure 10).
- The two axial cells are a vertex and an edge.
- The two axial cells are a vertex and a face (see Figure 8).
- The two axial cells are an edge and a face (see Figure 9).

Our situation is easier. In fact, suppose that the two axial cells are vertices, then by connectedness of a tree, there is a path between these two vertices. But by symmetry of the map, if such a path exists, it must exist in as many copies as the order of the symmetry (therefore at least twice). This implies that the map has at least two faces, which is in contradiction with the definition of a tree. In conclusion, the two axial cells cannot both be vertices.

By a similar argument, we prove that the four first situations described earlier are impossible. So, the only cases we have to consider here are the vertex–face and edge–face pairs. Now we study each case separately.

(1) The two axial cells are a vertex and a face.

In this case, it is simple to see that the quotient map of an l-rooted tree with n edges is a rooted tree with n/l edges and a distinguished face and vertex (the axial ones). In conclusion, as we have $(n/l+1)$ choices of distinguished vertex,

$$T_l'(n) = \frac{1}{n/l+1}\binom{2n/l}{n/l} \times (n/l+1) = \binom{2n/l}{n/l}.$$

(2) The two axial cells are an edge and a face.

In this case, we must consider a 2-rooted tree with n edges. The quotient action will divide an edge and share the other $n-1$ edges into two equal sets. So, if n is even, this quotient is impossible, and $T_e'(n) = 0$. Now we suppose that n is odd; then the two following situations can appear.

- The axial edge is not the root edge. In this case, the quotient map is simply a rooted tree with $(n-1)/2$ edges with an added half-edge (the axial one). Now we have just to notice that the number of ways to add a half-edge from a particular vertex is equal to the number of edges leaving this vertex. So there are exactly $(n-1)$ ways to add a half-edge from a rooted tree with $(n-1)/2$ edges.
- The axial edge is the root edge. In this case, the quotient map is a tree with $(n-1)/2$ edges and a rooted half-edge. By rooting the first edge to the left of the rooted half-edge, preserving the root vertex, we construct a bijection between these quotient maps and the set of rooted trees with $(n-1)/2$ edges (see Figure 12 for an example).

So, if n is odd,

$$\begin{aligned} T_e'(n) &= \frac{1}{(n-1)/2+1}\binom{n-1}{(n-1)/2} \times (n-1) + \frac{1}{(n-1)/2+1}\binom{n-1}{(n-1)/2} \\ &= \binom{n}{(n-1)/2}. \end{aligned}$$

https://doi.org/10.1017/etds.2013.100 Published online by Cambridge University Press

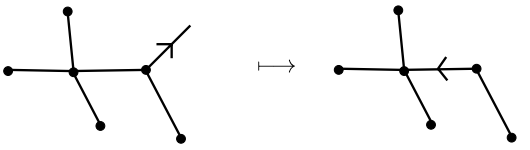


FIGURE 12. Example of equivalence between a tree with a rooted half-edge and a rooted tree.

This completes the enumeration of unrooted trees with n edges.

Now, to complete the proof of Theorem 4.3, we just need to estimate the growth of the sequence (σ_n), i.e. to prove the following result.

COROLLARY 4.4.

$$\lim_{n\to+\infty} (\sigma_n)^{1/n} = 4.$$

Proof. This corollary is a direct consequence of the last result. In fact, from the formula for σ_n, it is easy to prove that

$$\frac{1}{2n}\frac{1}{n+1}\binom{2n}{n} \le \sigma_n \le \frac{1}{n+1}\binom{2n}{n},$$

and so

$$\lim_{n\to+\infty} (\sigma_n)^{1/n} = \lim_{n\to+\infty} \left(\frac{1}{n+1}\binom{2n}{n}\right)^{1/n}.$$

Then, by using the Stirling formula, we can show that

$$\frac{1}{n+1}\binom{2n}{n} \sim \frac{1}{\sqrt{\pi}}\frac{4^n}{n^{3/2}},$$

in the sense that the quotient of the two terms tends to 1 as n tends to ∞. From this equivalence, we deduce the required result. □

4.3. *Enumeration of rooted generalized trees.* As in the previous example, we will use Theorem 4.3 to give an enumeration in the general case. But to use Theorem 4.3, we need to enumerate the set of rooted generalized trees (or equivalently the set of valid bracketing). We need to use the Lagrange–Bürmann inversion theorem (4.6), to demonstrate the following lemma.

LEMMA 4.5. *Denote by b_n the number of valid bracketings in a string of n elements. Then,*

$$b_{2n} = p_n = \sum_{k\ge 0} \frac{(-2n)_k(-n)_k}{(2)_k}\frac{2^k}{k!}, \quad n \ge 0$$

$$b_{2n-1} = q_n = \frac{1}{n}\sum_{k=0}^{n-1}\binom{2n}{k}\binom{n}{n-1-k}2^k, \quad n \ge 1,$$

with $(x)_n = x\cdot(x+1)\cdots(x+n-1)$ and $(x)_0 = 1$.

Proof. Consider a valid bracketing in a string of n elements, and read it from left to right. Two different situations appear in the beginning.

https://doi.org/10.1017/etds.2013.100 Published online by Cambridge University Press

Case 1. The first element in the string is a dot, and the bracketing representation composed by the other $n-1$ elements is a valid one.

Case 2. The first element in the string is a left square (respectively round) bracket, and so it is paired with the jth element of the string (with j even). Then the bracketing representation, thanks to the elements from 2 to $j-1$ and the elements from $j+1$ to n, is valid bracketing too.

So we deduce for these observations that b_n satisfies the recursion equation

$$b_n = b_{n-1} + 2 \sum_{2\alpha+\beta+2=n} b_{2\alpha} b_\beta, \quad n \geq 1 \text{ and } \alpha, \beta \geq 0,$$

where the first term of the sum is deducted from Case 1 and the second from Case 2. By convention, we set $b_0 = p_0 = 1$ and $q_0 = 0$. Now we consider the generating functions

$$p(z) = \sum_{n\geq 0} p_n z^n,$$
$$q(z) = \sum_{n\geq 0} q_n z^n.$$

Then by the recursive formula, we deduce for $n \geq 1$

$$\begin{aligned} p_n := b_{2n} &= b_{2n-1} + 2 \sum_{2\alpha+\beta=2n-2} b_{2\alpha} b_\beta \\ &= b_{2n-1} + 2 \sum_{k=0}^{n-1} b_{2k} b_{2(n-1-k)} \\ &= q_n + 2 \sum_{k=0}^{n-1} p_k p_{n-1-k} \end{aligned}$$

and

$$\begin{aligned} q_n := b_{2n-1} &= b_{2n-2} + 2 \sum_{2\alpha+\beta=2n-3} b_{2\alpha} b_\beta \\ &= b_{2(n-1)} + 2 \sum_{k=0}^{n-1} b_{2k} b_{2(n-1-k)-1} \\ &= p_{n-1} + 2 \sum_{k=0}^{n-1} p_k q_{n-1-k}. \end{aligned}$$

So, from these two equations one can deduce that

$$p = 1 + q + 2zp^2,$$
$$q = zp + 2zpq.$$

From the second equation, we obtain

$$p = \frac{q}{z(1+2q)},$$

https://doi.org/10.1017/etds.2013.100 Published online by Cambridge University Press

and so substituting this in the first equation, and after some simplifications, we get

$$q(1+2q) = z(1+q)(1+2q)^2 + 2q^2,$$

or

$$q = z(1+q)(1+2q)^2.$$

Then we use the following theorem.

THEOREM 4.6. (Lagrange–Bürmann inversion theorem) *Let $\phi(u)$ be a formal power series with $\phi_0 \neq 0$ and let $Y(z)$ be the unique formal power series solution of the equation $Y = z \cdot \phi(Y)$. Then the coefficient of $Y(z)$ of order n, denoted by $[z^n]Y(z)$, is given by*

$$[z^n]Y(z) = \frac{1}{n}[u^{n-1}]\phi(u)^n.$$

By using this theorem in our situation, setting $Y(z) = q(z)$ and $\phi(Y) = (1+Y)(1+2Y)^2$, we get

$$\begin{aligned} q_n = [z^n]q(z) &= \frac{1}{n}[u^{n-1}]((1+u)(1+2u)^2)^n \\ &= \frac{1}{n}\sum_{k=0}^{n-1}\binom{2n}{k}2^k\binom{n}{n-1-k}. \end{aligned}$$

Thanks to the Lagrange–Bürmann inversion theorem and equations verified by the generating functions p and q, we find also that

$$p_n = \sum_{k\geq 0}\frac{(-2n)_k(-n)_k}{(2)_k}\frac{2^k}{k!}.$$

The formula for p_n has been proved in the article of Dias [**Dia13**]. □

4.4. *Enumeration of unrooted generalized trees.* In the following, in order to simplify the notation, we set

$$p_{n,k} = \frac{(-2n)_k(-n)_k}{(2)_k}\frac{2^k}{k!}.$$

Notice that $p_{n,k}$ is equal to the number of rooted generalized trees of order n with k edges, $k+1$ vertices and $2(n-k)$ half-edges.

Now, we can prove the main result of this section as follows.

THEOREM 4.7. *Denote by p_n^+ the number of topologically different complex polynomial vector fields of degree $d = n+1$, then*

$$p_n^+ = \frac{1}{2n}\left[p_n + \sum_{\substack{l\geq 2\\ l\mid 2n}}\varphi(l)\cdot\begin{cases}\displaystyle\sum_{k\geq 0}p_{n/l,k}\cdot(k+1) & \text{if } 2n/l \text{ is even}\\ c_{2n/l} & \text{if } 2n/l \text{ is odd}\end{cases}\right.$$

$$\left. + \begin{cases}0 & \text{if } n \text{ is even}\\ 2n\cdot p_{(n-1)/2} & \text{if } n \text{ is odd}\end{cases}\right], \quad n\geq 1,$$

https://doi.org/10.1017/etds.2013.100 Published online by Cambridge University Press

$\deg = n+1$	p_n^+
2	3
3	6
4	26
5	123
6	801
7	5686
8	43846
9	353987
10	2968801
11	25605445

FIGURE 13. The first 10 values of p_n^+.

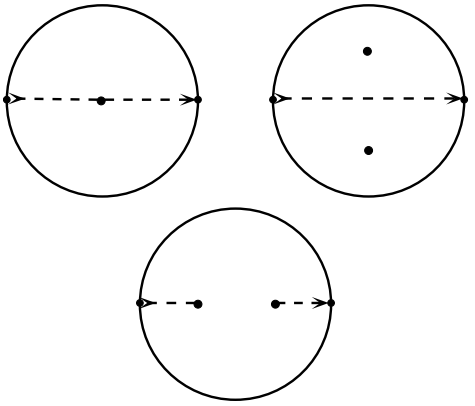


FIGURE 14. Modelization of the three polynomial vector fields of degree two.

with c_m satisfying the recursive formula

$$c_m = c_{m-1} + 2 \sum_{2\alpha+\beta+2=m} b_{2\alpha} c_\beta + 2 \sum_{2\alpha+\beta+3=m} c_{2\alpha+1} b_\beta, \quad m \geq 1,$$
$$c_0 = 1.$$

We will give in the next subsection an explicit formula for the coefficient c_m. The first values obtained by this formula are given in Figure 13, and modelizations of the polynomial vector fields of degree two and three are given in Figures 14 and 15.

Proof. By adapting Theorem 4.3 in our situation, we can write

$$p_n^+ = \frac{1}{2n}\left[p'(n) + \sum_{\substack{l \geq 2 \\ l \mid 2n}} \varphi(l) \cdot p'_l(n) + p'_e(n) \right], \quad n \geq 2.$$

Moreover, by Lemma 4.5, we still have $p'(n) = p_n$, so we just need to determine the values of $p'_e(n)$ and $p'_l(n)$.

https://doi.org/10.1017/etds.2013.100 Published online by Cambridge University Press

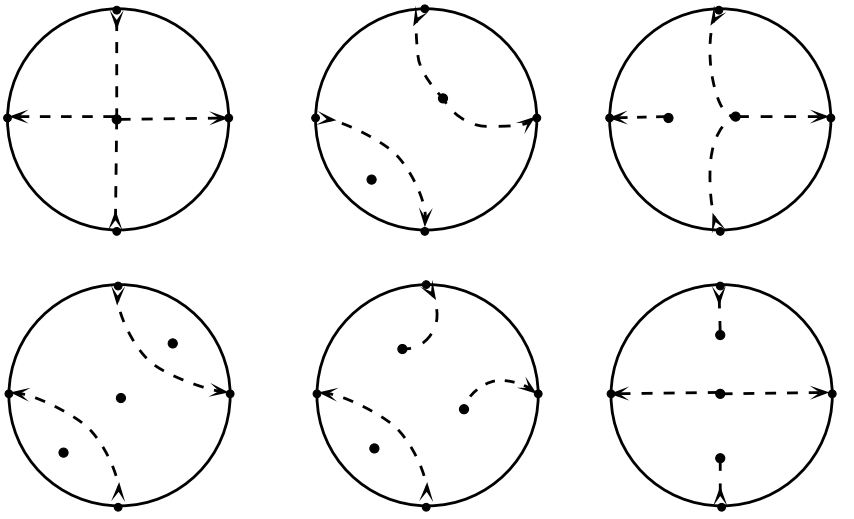


FIGURE 15. Modelization of the six polynomial vector fields of degree three.

For that, we need to study the quotient maps and their respective pairs of axial cells. As in the example of trees, and by the same argument, there are only two different pairs of axial cells: the vertex–face pair and the edge–face pair. Now we study each case separately.

(1) The two axial cells are an edge and a face (cf. Figure 16). In this case, the symmetry we consider is necessarily of order two, so we need to consider 2-rooted generalized trees. Moreover, to be in this situation it is necessary that n is odd. In fact, as we have a symmetry of order two and as no vertex is axial, then the number of vertices is necessarily even, and so the number of edges is necessarily odd. Moreover, by definition of a rooted generalized tree, the number of half-edges in each vertex is also even, so we deduce that the number n, which is equal to the number of edges plus half of the number of half-edges, is necessarily odd. In conclusion,

$$p'_e(n) = 0 \quad \text{if } n \text{ is even.}$$

Suppose now that n is odd, we need to distinguish two possible situations as in the case of trees (see §4.2).

- The axial edge does not contain the roots of the map. In this case, the quotient map is a rooted generalized tree with an added distinguished half-edge, and as in the case of trees, we have exactly $(n-1)$ ways to add a distinguished half-edge. Moreover, the axial edge may be of two types (continuous or dotted), so the number of maps in this situation is equal to
$$p_{(n-1)/2} \times (n-1) \times 2.$$
- The axial edge contains the two roots of the map. In this case, the quotient map is an unrooted generalized tree, to which we must add to a vertex a distinguished isolated half-edge. Moreover, this distinguished half-edge becomes the root of the quotient map. So, by transcribing the information into a bracketed representation, we obtain a valid bracketing in a string of n elements containing the integers from 0 to $n-1$.

https://doi.org/10.1017/etds.2013.100 Published online by Cambridge University Press

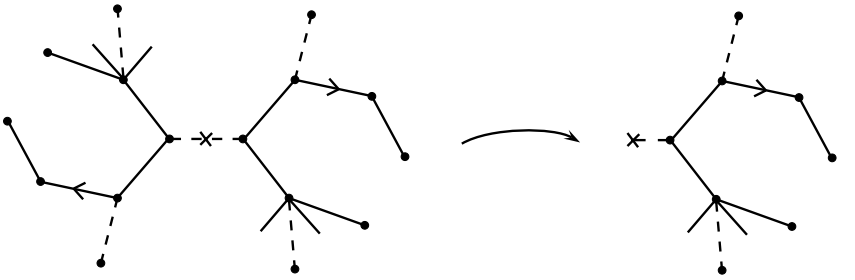


FIGURE 16. Example of a 2-rooted generalized tree and its quotient map in the case where the two axial cells are an edge and a face.

Moreover, the element zero is not paired with another number, because the root of the map is an isolated half-edge, so we can erase the element zero to obtain a valid bracketing in the string $\{1, \ldots, n-1\}$.

In conclusion, the set of quotient maps obtained in this case from rooted generalized trees having n half-edges is in bijection with the set of rooted generalized trees of order $(n-1)/2$ times $\{0, 1\}$, as the axial edge may be of two types (continuous or dotted). So the number of maps in this situation is equal to

$$2 \cdot p_{(n-1)/2}.$$

Finally, if n is odd,

$$p'_e(n) = 2(n-1) \cdot p_{(n-1)/2} + 2 \cdot p_{(n-1)/2} = 2n \cdot p_{(n-1)/2}.$$

(2) The two axial cells are a vertex and a face. In this case, the order of the symmetry is equal to $l \geq 2$, and the maps considered are l-rooted generalized trees. As in the previous case, it will be necessary to distinguish two situations.

- If $2n/l$ is even, then it is simple to see that the quotient map is a rooted generalized tree of order $2n/l$ with a distinguished vertex (see Figure 17 for an example). By Lemma 4.5, and as $p_{n,k}$ is equal to the number of rooted generalized trees of order n with k edges, we deduce that

$$p'_l(n) = \sum_{k \geq 0} p_{n/l,k} \cdot (k+1).$$

- If $2n/l$ is odd, then the situation becomes more difficult in the sense that the quotient map is not necessarily a generalized tree (see Figure 18 for an example). To achieve an enumeration in this situation, we will return to a bracketing problem by interpreting this one as follows: a bracketing representation of this problem comes from a valid bracketing with an added dot anywhere in the string.

  For example, from the valid bracketing [[ ]] we can construct [[•]] as a bracketing representation of our problem. These bracketing representations are called *quasi-valid bracketing*, and the number of quasi-valid bracketing in a string of m elements is denoted by c_m.

  Now consider a quasi-valid bracketing in a string of m elements; three situations can occur.

https://doi.org/10.1017/etds.2013.100 Published online by Cambridge University Press

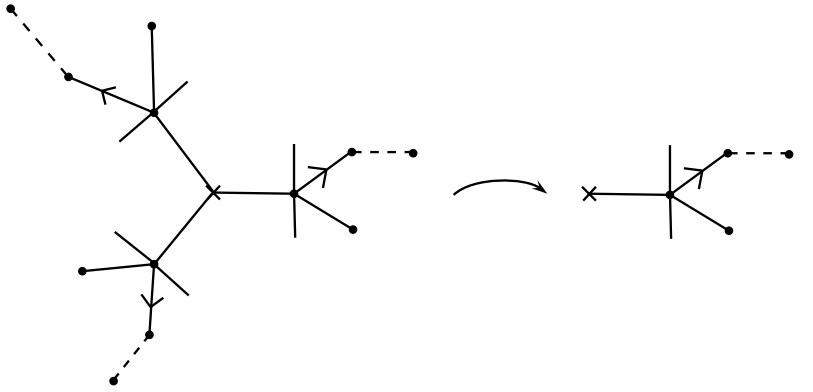


FIGURE 17. Example of a 3-rooted generalized tree and its quotient map in the case where the two axial cells are a vertex and a face (case $2n/l$ even).

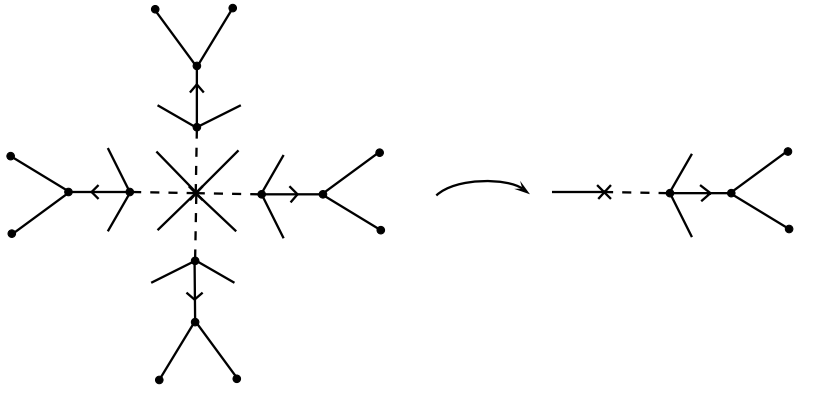


FIGURE 18. Example of a 4-rooted generalized tree and its quotient map in the case where the two axial cells are a vertex and a face (case $2n/l$ odd).

- The first element is a dot. In this case, the bracketing representation obtained by deleting the first element of the initial string is a quasi-valid bracketing.
- The first element is a left (square or round) bracket and its associated right bracket is the jth element of the string, with j even. In this case, the string containing the elements from 2 to $j-1$ is a valid bracketing, and the string containing the integers from $j+1$ to m is a quasi-valid bracketing.
- The first element is a left (square or round) bracket and its associated right bracket is the kth element of the string, with k odd. In this case, the string containing the integers from 2 to $k-1$ is a quasi-valid bracketing, and the bracketing representation in the string containing the integers from $k+1$ to m is a valid bracketing.

In conclusion, c_m satisfies the following recurrence relation:

$$c_m = c_{m-1} + 2 \sum_{2\alpha+\beta+2=m} b_{2\alpha} c_\beta + 2 \sum_{2\alpha+\beta+3=m} c_{2\alpha+1} b_\beta. \tag{3}$$

This completes the proof of the theorem. □

https://doi.org/10.1017/etds.2013.100 Published online by Cambridge University Press

COROLLARY 4.8.

$$\lim_{n\to+\infty}(p_n^+)^{1/n}=\frac{2}{5\sqrt{5}-11}\approx 11.09.$$

Proof. Thanks to Theorem 4.7, it is easy to see that

$$\frac{1}{2n}p_n\le p_n^+\le p_n.$$

So, by using the result proved by Dias in [**Dia13**], we deduce that

$$\lim_{n\to+\infty}(p_n^+)^{1/n}=\lim_{n\to+\infty}(p_n)^{1/n}=\frac{2}{5\sqrt{5}-11}.$$ □

4.5. *A closed form of c_m.* In order to complete the proof of Theorem 1.2, it only remains to give a closed formula for the coefficients c_m. For that, we try to use the same method as before (cf. Lemma 4.5) by manipulating the generating functions somewhat. To start, set

$$r_m := c_{2m},$$
$$s_m := c_{2m+1}.$$

Then, using the recurrence relation (3) satisfied by c_m, we deduce

$$\begin{aligned} r_m := c_{2m} &= c_{2m-1}+2\sum_{j=0}^{m-1}b_{2j}c_{2m-2j-2}+2\sum_{j=0}^{m-2}b_{2m-2j-3}c_{2j+1}\\ &= s_{m-1}+2\sum_{j=0}^{m-1}p_j r_{m-j-1}+2\sum_{j=0}^{m-2}q_{m-j-1}s_j \end{aligned}$$

and

$$\begin{aligned} s_m := c_{2m+1} &= c_{2m}+2\sum_{j=0}^{m-1}b_{2j}c_{2m-2j-1}+2\sum_{j=0}^{m-1}b_{2m-2j-2}c_{2j+1}\\ &= c_{2m}+4\sum_{j=0}^{m-1}b_{2m-2j-2}c_{2j+1}\\ &= r_m+4\sum_{j=0}^{m-1}p_{m-j-1}s_j. \end{aligned}$$

So, let us consider the generating functions

$$p(z)=\sum_{n\ge0}p_n z^n,\quad q(z)=\sum_{n\ge0}q_n z^n$$

as before and

$$r(z)=\sum_{n\ge0}r_n z^n,\quad s(z)=\sum_{n\ge0}s_n z^n.$$

These four functions satisfy the following equations:

$$p(z)=1+q(z)+2zp(z)^2, \tag{4}$$
$$q(z)=zp(z)+2zp(z)q(z), \tag{5}$$
$$r(z)=1+zs(z)+2zp(z)r(z)+2zq(z)s(z), \tag{6}$$
$$s(z)=r(z)+4zp(z)s(z). \tag{7}$$

https://doi.org/10.1017/etds.2013.100 Published online by Cambridge University Press

Notice already that the last equation can be used to determine the coefficients r_m of the function r in terms of those of s and p. More precisely,

$$r_m = s_m - 4\sum_{j=0}^{m-1} p_{m-j-1}s_j. \tag{8}$$

Thus, we only need to determine the coefficients s_m of the function s to complete our enumeration. For that, we note that by multiplying equation (4) by r, equation (6) by p and by identifying the results, we obtain

$$p + zsp + 2zqsp + 2zrp^2 = r + qr + 2zrp^2.$$

So, after a simplification, and noticing that $sq = zsp + 2zsqp$, we deduce that

$$p + sq = r + rq.$$

Then, as $sq = rq + 4zpsq$, we obtain

$$p + 4zpsq = r.$$

Thanks to equations (5) and (7), we can conclude that

$$s(1 - 2zp - 2q) = p,$$

which we can still write as

$$s(4\tilde{p}^2 - 6\tilde{p} + 1) = p(1 - 2zp) \quad \text{with } \tilde{p} = zp. \tag{9}$$

So, for now, we need to determine the function $(4\tilde{p}^2 - 6\tilde{p} + 1)^{-1}$ in order to give an explicit formula for the coefficients of s. Note that by using equations (4) and (5) one may easily check that

$$4z^2p^3 - 4zp^2 + (z + 1)p - 1 = 0,$$

so

$$4\tilde{p}^3 = 4\tilde{p}^2 - (z + 1)\tilde{p} + z.$$

We can hope from this relation to determinate some (rational) coefficients u, v, w such that

$$(u\tilde{p}^2 + v\tilde{p} + w)(4\tilde{p}^2 - 6\tilde{p} + 1) = 1.$$

After some calculations, we obtain a positive result given by the following relations:

$$u = \frac{-4(z + 3)}{z^2 + 11z - 1},$$
$$v = \frac{10}{z^2 + 11z - 1},$$
$$w = \frac{-(z^2 + 5z + 1)}{z^2 + 11z - 1}.$$

From this result, and equation (9), we obtain

$$(z^2 + 11z - 1)s = p(1 - 2zp)[-4(z + 3)z^2p^2 + 10zp - (z^2 + 5z + 1)]$$

https://doi.org/10.1017/etds.2013.100 Published online by Cambridge University Press

and so after simplification

$$(z^2 + 11z - 1)s = 2z(3z - 1)p^2 + (2z + 1)p + (z - 2). \tag{10}$$

However, the function $2z(3z - 1)p(z)^2 + (2z + 1)p(z) + (z - 2)$ can be written as a formal series with coefficients in $\mathbb{R}$, so there exist coefficients $a_n \in \mathbb{R}$ such that

$$2z(3z - 1)p(z)^2 + (2z + 1)p(z) + (z - 2) = \sum_{n\geq 0} a_n z^n.$$

Then we have $a_0 = -1$, $a_1 = 4$ and for $n \geq 2$

$$\begin{aligned} a_n &= 6\sum_{k=0}^{n-2} p_k p_{n-k-2} - 2\sum_{k=0}^{n-1} p_k p_{n-k-1} + 2p_{n-1} + p_n \\ &= 6\sum_{k=0}^{n-2} p_k p_{n-k-2} - 2\sum_{k=0}^{n-2} p_k p_{n-k-1} + p_n. \end{aligned}$$

Finally,

$$(z^2 + 11z - 1)^{-1} = \sum_{n\geq 0}\left(\sum_{k=0}^{n} -\alpha^k \beta^{n-k}\right) z^n,$$

where α and β are the roots of the polynomial $X^2 + 11X - 1$.

We conclude from equation (10) and the last results that

$$c_{2m+1} := s_m = -\sum_{k=0}^{m} a_k \left(\sum_{i=0}^{m-k} \alpha^i \beta^{m-k-i}\right),$$

and from equation (8) that

$$\begin{aligned} c_{2m} := r_m &= s_m - 4\sum_{j=0}^{m-1} p_{m-j-1} s_j \\ &= c_{2m+1} - 4\sum_{j=0}^{m-1} c_{2j+1} p_{m-j-1}. \end{aligned}$$

This completes the proof of the main result of this article. □

Acknowledgements. I am grateful to Tan Lei for introducing the subject, useful conversations and a careful reading of this work during its preparation. I am also grateful to Kealey Dias for her help in the finalization of this paper.

References

[AGP10] M. J. Alverez, A. Gasull and R. Prohens. Topological classification of polynomial complex differential equations with all the critical points of centre type. *J. Difference Equ. Appl.* **16** (2010), 411–423.

[BD10] B. Branner and K. Dias. Classification of complex polynomial vector fields in one complex variable. *J. Difference Equ. Appl.* **16** (2010), 463–517.

https://doi.org/10.1017/etds.2013.100 Published online by Cambridge University Press

[BM96] S. Benchekroun and P. Moszkowski. A new bijection between ordered trees and legal bracketings. *European J. Combin.* **17** (1996), 605–611.

[Dav12] T. Davis. Catalan numbers, 2012, http://geometer.org/mathcircles/catalan.pdf.

[Dia13] K. Dias. Enumerating combinatorial classes of the complex polynomial vector fields in $\mathbb{C}$. *Ergod. Th. & Dynam. Sys.* **33** (2013), 416–440.

[DES] A. Douady, F. Estrada and P. Sentenac. Champs de vecteurs polynômiaux sur $\mathbb{C}$, unpublished manuscript.

[Lis96] V. A. Liskovets. A reductive technique for enumerating non-isomorphic planar maps. *Discrete Math.* **156** (1996), 197–217.

[Lis98] V. A. Liskovets. Reductive enumeration under mutually orthogonal group actions. *Acta Appl. Math.* **52** (1998), 91–120.

[Lis04] V. A. Liskovets. Enumerative formulae for unrooted planar maps: a pattern. *Electron. J. Combin.* **11** (2004).

[Man71] P. Mani. Automorphismen von polyedrischen graphen. *Math. Ann.* **192** (1971), 279–303.

[Pil06] K. M. Pilgrim. Polynomial vector fields, dessins d'enfants, and circle packings. *Complex Dynamics (Contemporary Mathematics, 396)*. American Mathematical Society, Providence, RI, 2006.

https://doi.org/10.1017/etds.2013.100 Published online by Cambridge University Press